**Supplemental information**

# A glia-enriched stem cell 3D model of the human

# brain mimics the glial-immune

# neurodegenerative phenotypes of multiple sclerosis

Francesca Fagiani, Edoardo Pedrini, Stefano Taverna, Elena Brambilla, Valentina Murtaj, Paola Podini, Francesca Ruffini, Erica Butti, Clarissa Braccia, Annapaola Andolfo, Roberta Magliozzi, Lena Smirnova, Tanja Kuhlmann, Angelo Quattrini, Peter A. Calabresi, Daniel S. Reich, Gianvito Martino, Paola Panina-Bordignon, and Martina Absinta

**A** #945_hSox10
11.903 bp

**B** Transfection of 293T cells for lentiviral vector production → Transduction of target cells → Selection of infected cells with stable infection constructs

Transfer vector / Envelope vector / Packaging vector → Producer cells: HEK 293T → Lentiviral particles → Target cells: NPC → Cell sorting (FACS-gating of GFP⁺ cells)

**C** Organoids diameter (µm)

**D** ~150 organoids/well
6-well plate

**E** Doxycycline-induced GFP-SOX10

Day 1 ⟶ shaker ⟶ W2 ⟶ W8

+ doxycycline +AA, T3, rhNT3, rhPDGF, SAG, dbcAMP, IGF1 (3 days)

+ doxycycline +AA, T3, rhNT3, dbcAMP, IGF1 (11 days)

+ AA, T3, rhNT3, dbcAMP, IGF1, GDNF and BDNF

**F** Patch-clamp

**G** MAP2/SOX10/DAPI — W5 Neurons — 100 µm

**H** MAP2/SOX10/DAPI — W5 Neurons — W5

**I** NESTIN/SOX10/DAPI — W2 NPC — W8 — 100 µm — %Area (Nestin) W2 W5 W8 ****

**J** PAX6/SOX10/DAPI — W2 NPC — W8 — 100 µm — %Area (Pax6) W2 W5 W8 ***

**K** CD11B/CD45/DAPI — Day 34 2D hiMicroglia — 100 µm

**L** TMEM119/CD45/DAPI — Day 34 2D hiMicroglia — 100 µm

**M** IBA1/SOX10/DAPI — Day 1 post incorporation — Day 7 post incorporation — Day 7 post incorporation — 100 µm

**N** IBA1/DAPI — W9 hiMicroglia within organoid — 100 µm

**O** TMEM119/MAP2/MBP/DAPI — hiMicroglia within organoid — 100 µm

**P** IBA1/MBP/DAPI — Z-stack (hiMicroglia within organoid)

**Figure S1. SOX10-eGFP organoids' production and characterization by immunofluorescence. Related to Figure 1.**

(A) Lentiviral vector encoding the SOX10 coding sequence and GFP as reporter gene under the control of doxycycline-inducible promoter.

(B) Schematic for transfection of 293T HEK cells with transfer, envelope, and packaging vectors for lentiviral particles production, transduction of target cells (*i.e.,* NPCs) and selection of infected NPCs with stable infection constructs by FACS-gating of GFP$^+$ cells.

(C) Organoids' diameter ($\mu$m) over time (W=weeks) (*n*=10 organoids per time point).

(D) Representative image of organoids (*n* ~ 150 organoids) in a well of a 6-well-plate.

(E) Schematic for doxycycline-induced SOX10 induction during the 8-week protocol (see **STAR METHODS** for a detailed description).

(F) Electrophysiological organoid recording: example of action potential firing (black trace) in response to injection of a suprathreshold current step (50 pA, 500 ms; gray trace); representative trace showing an inward Na$^+$ (black arrowhead) and an outward K$^+$ current (white arrowhead) evoked by a voltage step from -70 to -10 mV (100 ms, gray trace); example of spontaneous postsynaptic currents (excerpted from a longer trace lasting 1 minute) recorded at -60 mV in voltage-clamp mode.

(G-H) Representative images of free-floating organoids exposed to doxycycline after 5 weeks of differentiation. Immunostaining of MAP$^+$ neurons and OPCs endogenously expressing SOX10. Nuclei are marked with DAPI.

(I) Immunostaining of NESTIN$^+$ and SOX10$^+$ cells (30X) out of DAPI in whole cryosections from 2- and 8-week-old organoids exposed to doxycycline and quantification of NESTIN$^+$ cells (% staining area) at 2, 5, and 8 weeks (one-way ANOVA and multiple comparison) (*n*=3).

(J) Immunostaining of PAX6$^+$ and SOX10$^+$ cells (30X) out of DAPI in whole cryosections from 2- and 8-week-old organoids exposed to doxycycline and quantification of PAX6$^+$ cells (% area) at 2, 5, and 8 weeks (*n*=3, one-way ANOVA and Tukey's multiple comparisons test, * p<0.05, ** p<0.01, *** p<0.001).

(K-L) Immunolabeling of CD11B$^+$, CD45$^+$(left: 30X), TMEM119$^+$ cells (right: 30X) in 2D culture of hiMicroglia at day 34 of differentiation. Nuclei are marked with DAPI.

(M) Immunolabeling of IBA1$^+$ and SOX10$^+$ cells (30X) out of DAPI in cryosections from 8- and 9-weeks-old organoids 1 day and 7 days after hiMicroglia incorporation.

(N-O) Immunolabeling of IBA1$^+$ hiMicroglia (left: 30X) and TMEM119$^+$/MBP$^+$/MAP2$^+$ cells (right: 30X) out of DAPI in whole cryosections from 9 weeks-old organoids.

(P) Z-stacks of IBA1$^+$ microglia and MBP$^+$ OL out of DAPI in whole cryosections from 9 weeks-old organoids.
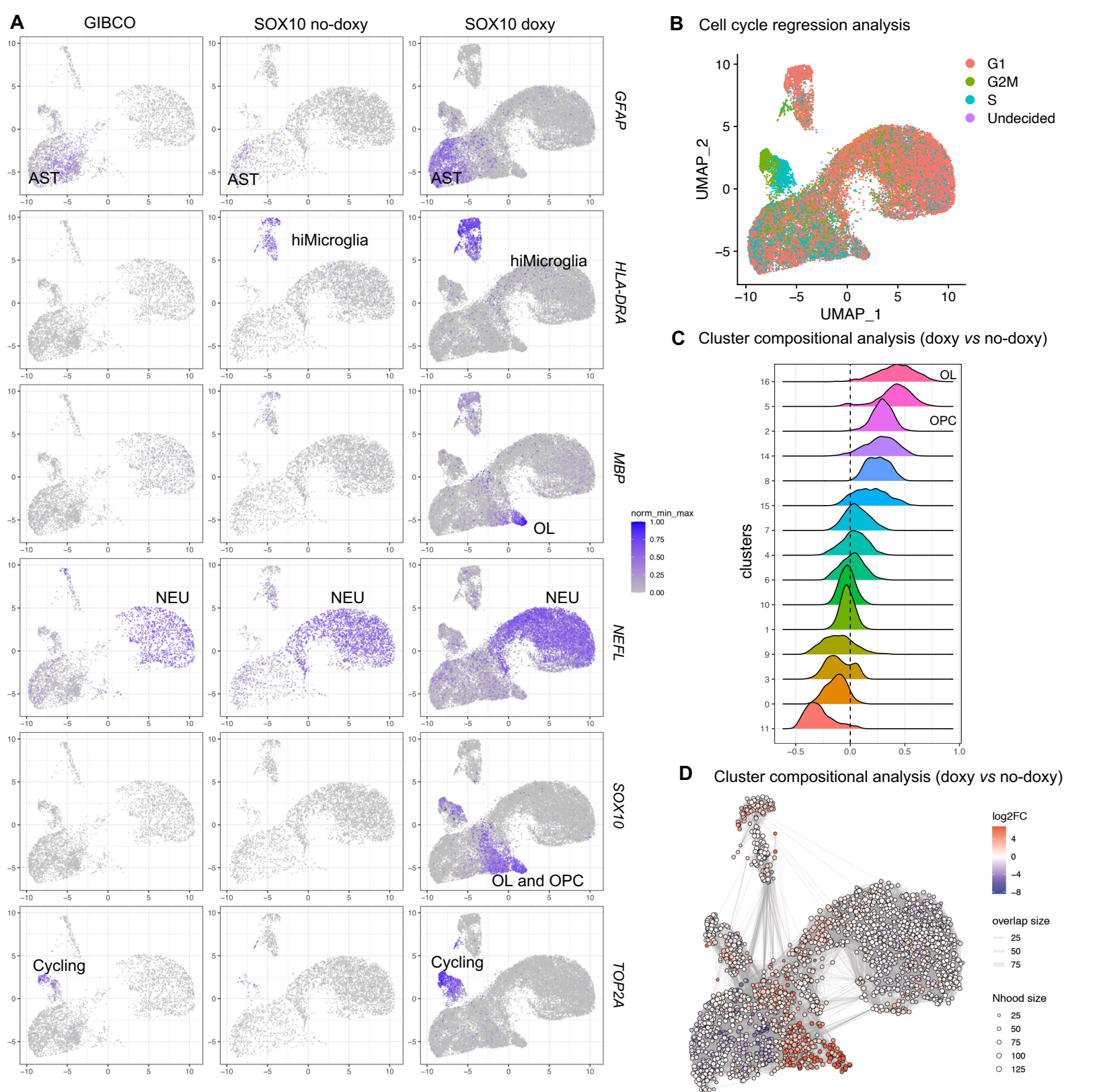
*Abbreviations:* NPCs: neural precursor cells.

**Synapses**
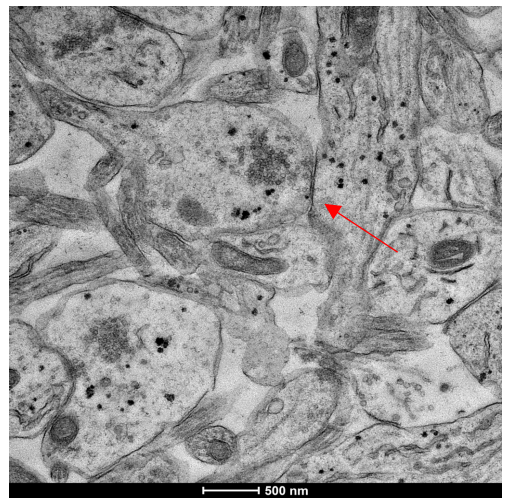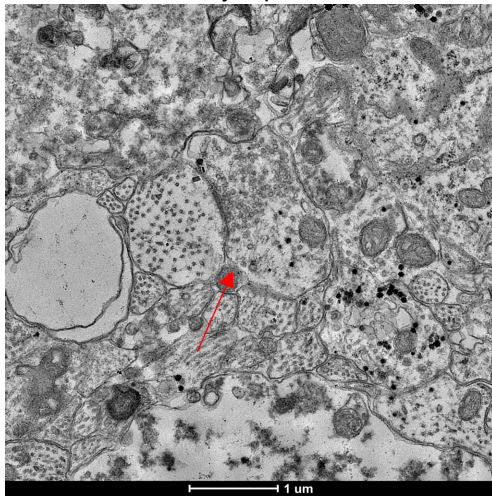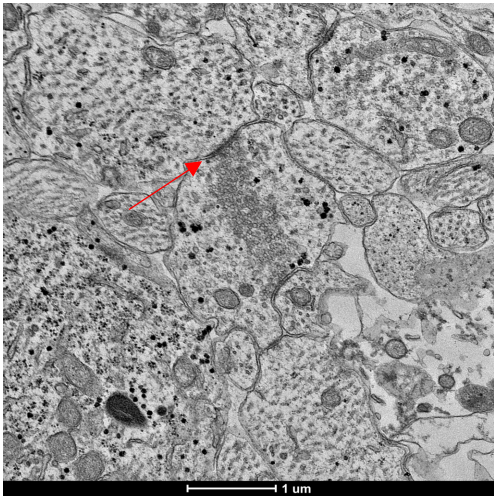
**Axons**
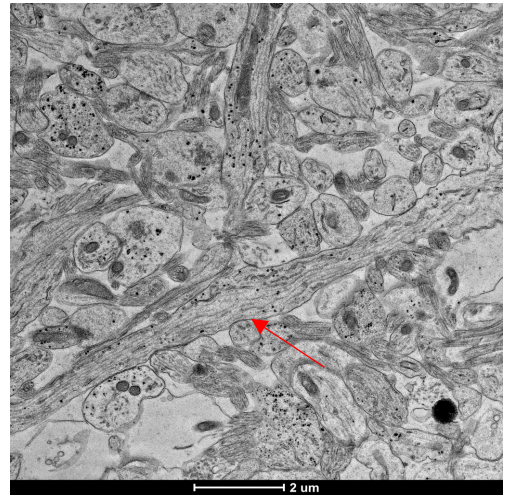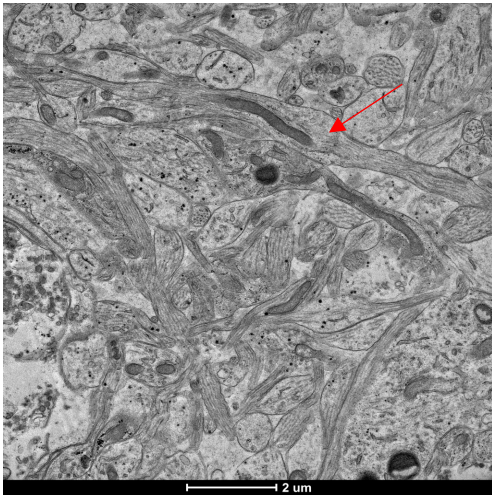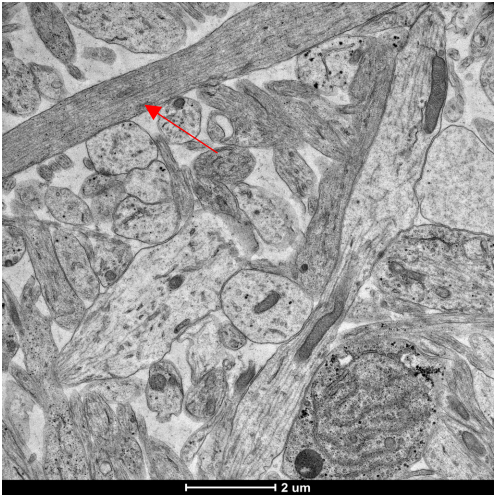
**Myelination stages**
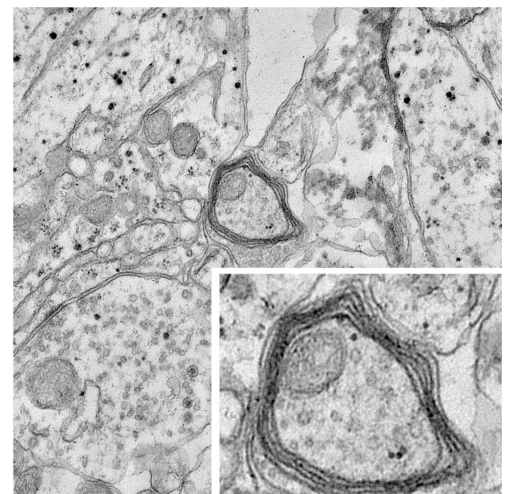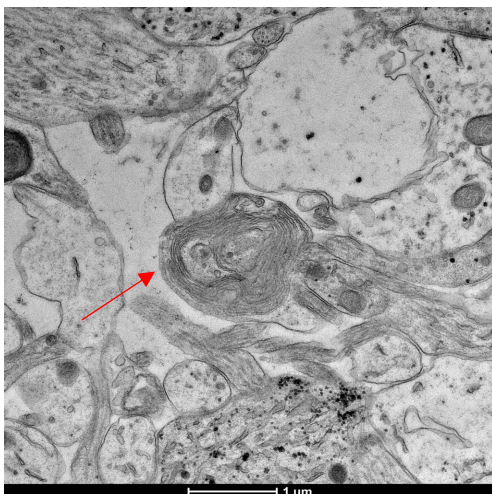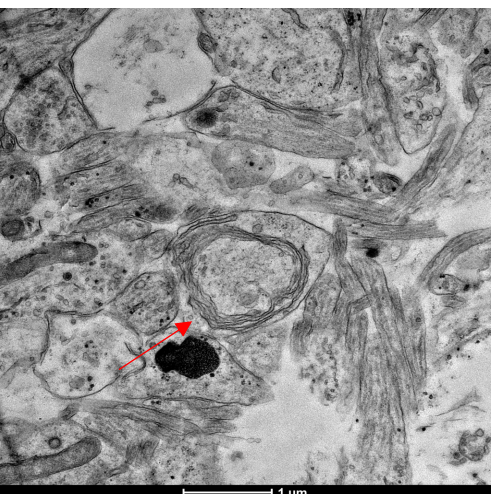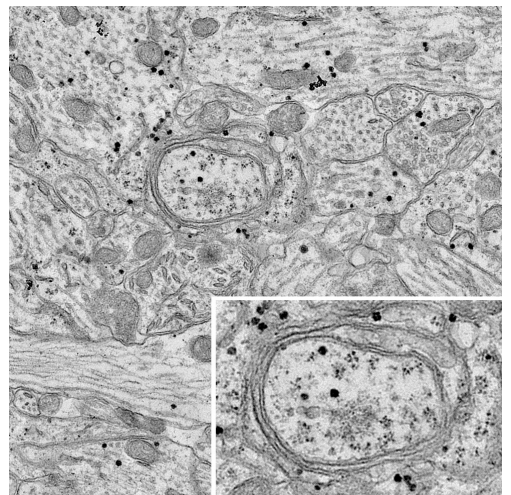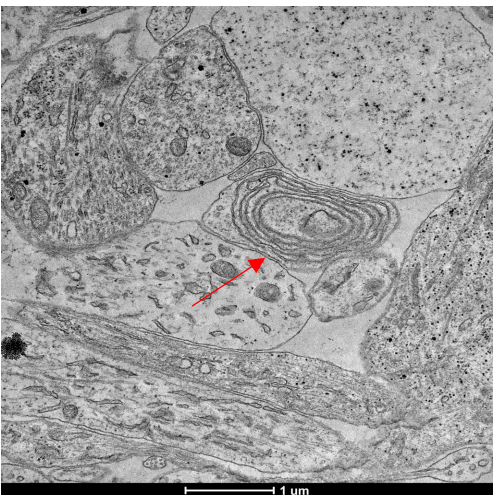
**Figure S2. Ultrastructure analysis on organoids. Related to Figure 1.**
(A-B) Ultrastructure analysis by electron microscopy at 8 weeks showed: (A) evidence of cell-to-cell junctions (red arrowhead) demonstrating functional interactions between the cells in doxycycline-treated organoids; (B) axonal projections (red arrowhead) in doxycycline-treated organoids.
(C) Transmission electron microscopy images of organoids showing early myelination processes during the differentiation protocol (2 and 5 weeks) to late time points (8 weeks). Electron microscopy was performed on organoids derived from 4 independent experiments with similar results.

**A** GIBCO / SOX10 no-doxy / SOX10 doxy — *GFAP*, *HLA-DRA*, *MBP*, *NEFL*, *SOX10*, *TOP2A*

norm_min_max

**B** Cell cycle regression analysis — G1, G2M, S, Undecided

**C** Cluster compositional analysis (doxy *vs* no-doxy) — OL, OPC

**D** Cluster compositional analysis (doxy *vs* no-doxy) — log2FC, overlap size, Nhood size

**E** MBP⁺ OLs in W16 organoids not exposed to doxycycline — MBP/DAPI, W16, 100 µm

**F** MBP⁺ OLs in W16 organoids exposed to doxycycline — MBP/DAPI, W16, 100 µm
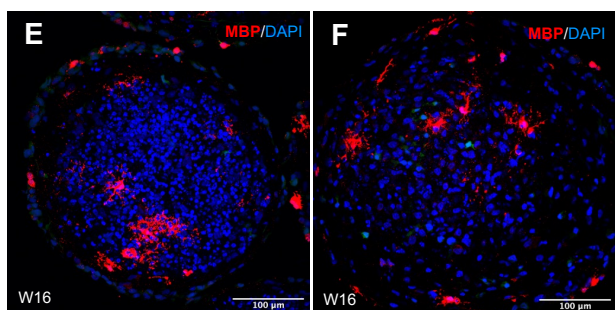
**G** SOX10-eGFP organoids onto the reference atlas — Reference atlas: adult, fetal; Prediction score
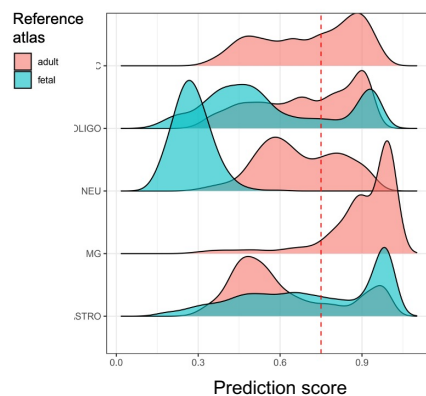
**H** Cortical organoids (Tanaka et al., 2020) onto the reference atlas — NEU, MG, ASTRO; Prediction score
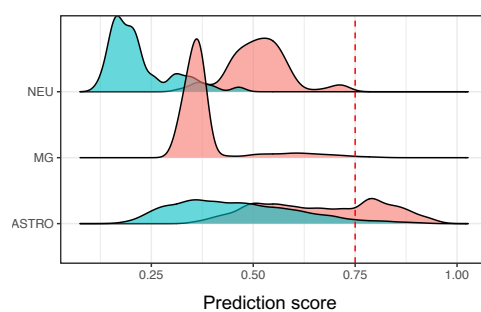
**Figure S3. Organoids' cell type and cluster composition. Related to Figure 2.**
(A) UMAP showing *GFAP*, *HLA-DRA*, *MBP*, *NEFL, SOX10* and *TOP2A* expression in organoids.
(B) Cell cycle regression analysis indicating cells in G1, G2M, and S phase.
(C) Organoids' cluster compositional analysis for the comparison exposed *vs* not exposed to doxycycline: using Cacoa algorithm, the statistical significance of loading coefficients is reached for clusters 16, 2, 15, 7, 8, 5, and 1.
(D) Organoids' cluster compositional analysis for the comparison exposed *vs* not exposed to doxycycline: using MiloR, the density plot of the neighbors shows that the oligolineage clusters are significantly denser in doxycycline-stimulated organoids.
(E-F) Immunostaining of MBP⁺ OL (30X) out of DAPI in whole cryosections from 16-week-old organoids not exposed to doxycycline *vs* organoids exposed to doxycycline.
(G-H) SOX10-organoids (G) and human cortical organoids (scRNAseq dataset metanalysis from Tanaka et al.) scRNAseq data were mapped on the human adult vs fetal reference atlases. The distribution of the mapping prediction scores is shown separately for adult (pink) *vs* fetal (cyan) atlas. The red dotted line indicates the prediction scores above 0.75, indicating high confidence supported by multiple consistent gene anchors.

*Abbreviations:* NEU: neurons; ASTRO: astrocytes; OPC: oligodendrocyte precursor cells; OL: oligodendrocytes; CYCLING: cycling cells.

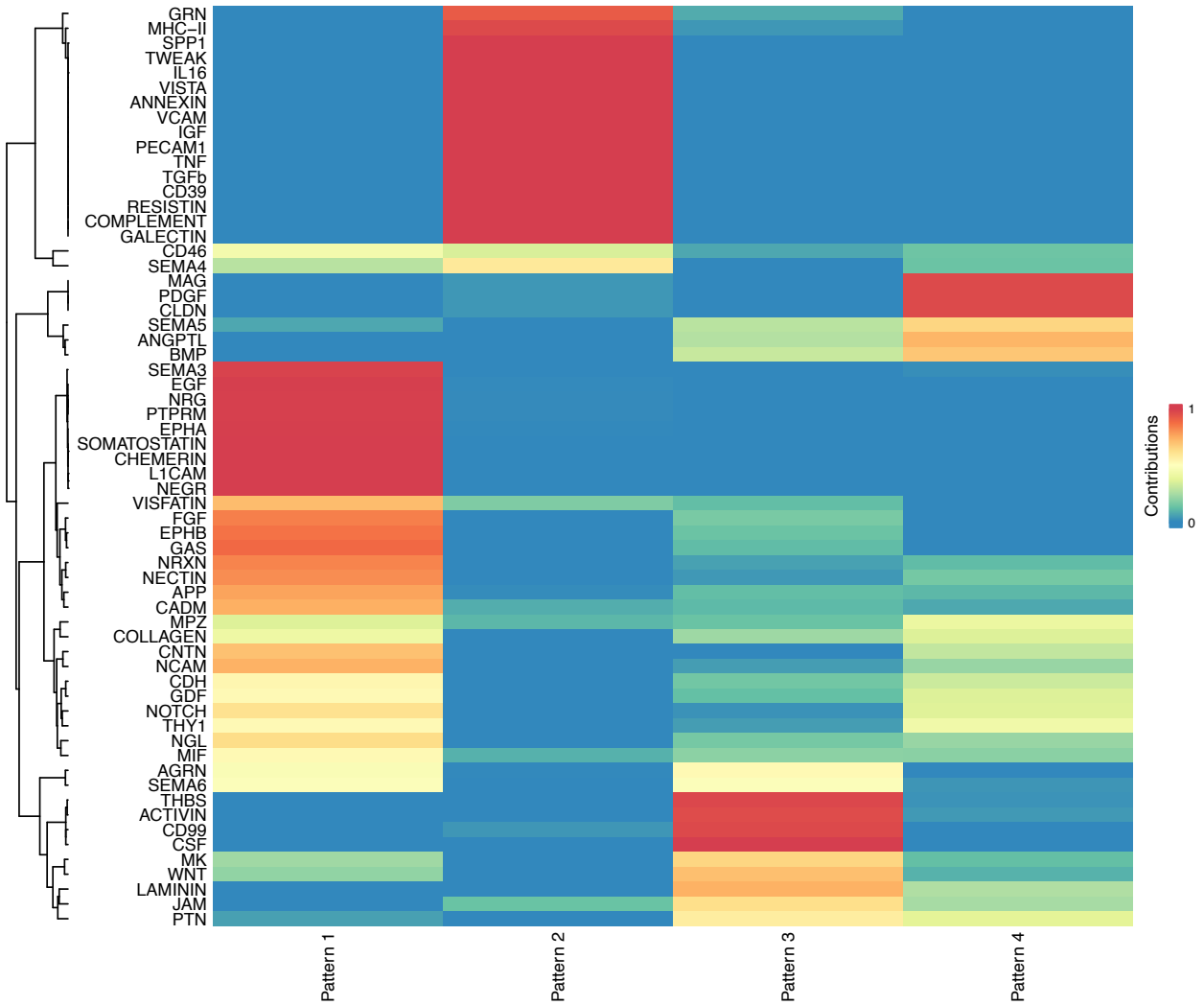**A** Outgoing communication patterns of secreting cells
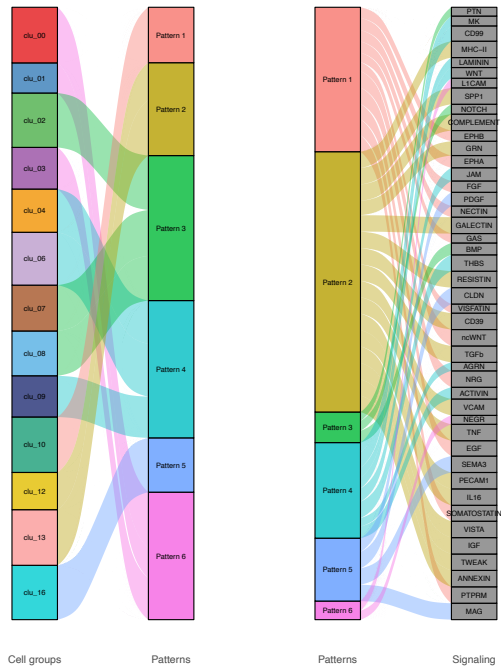
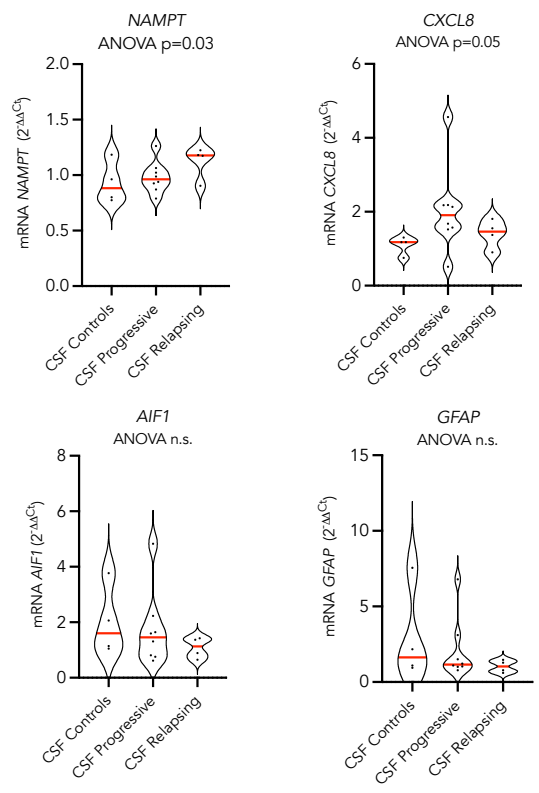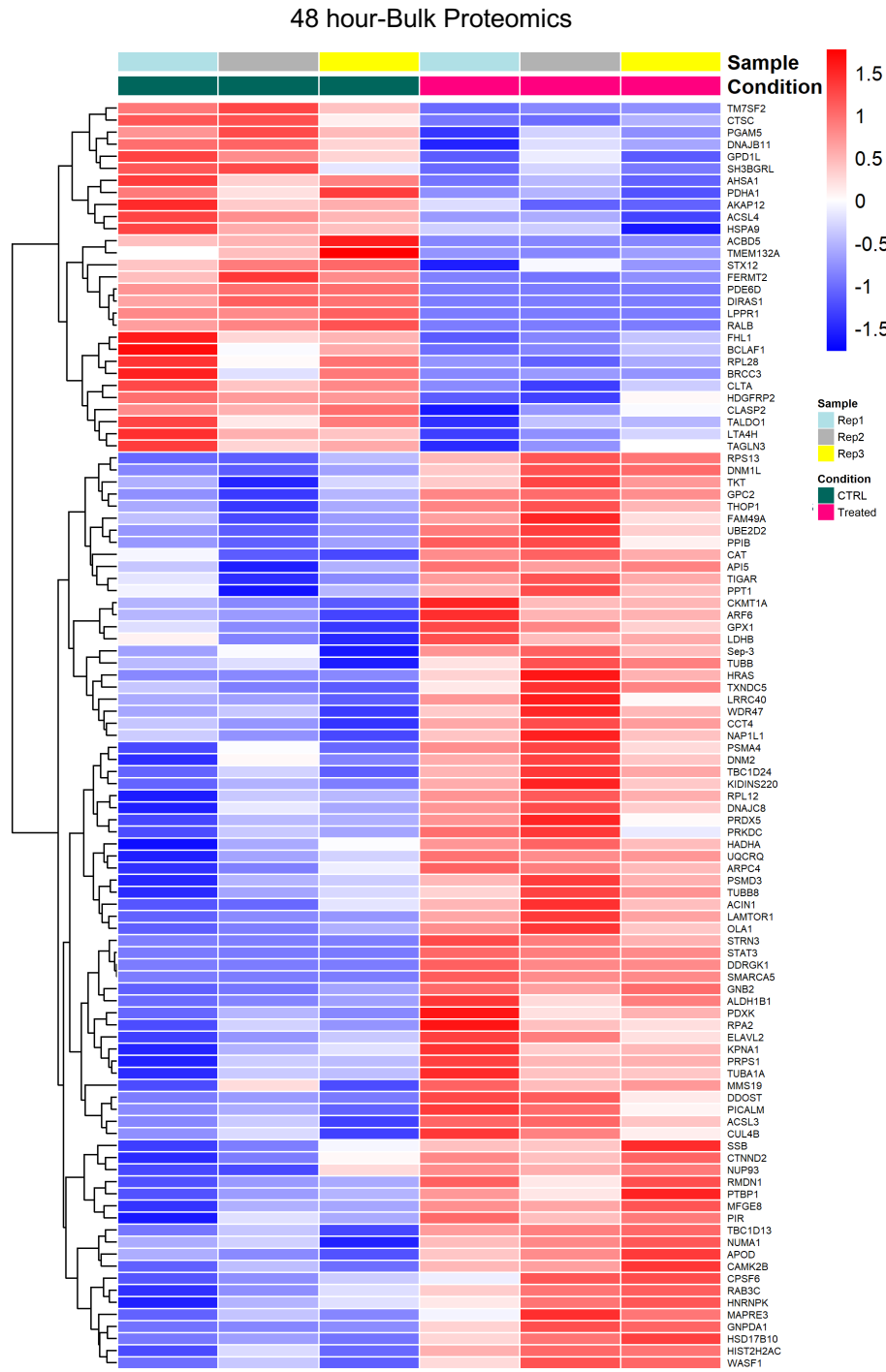**B** Incoming communication patterns of secreting cells
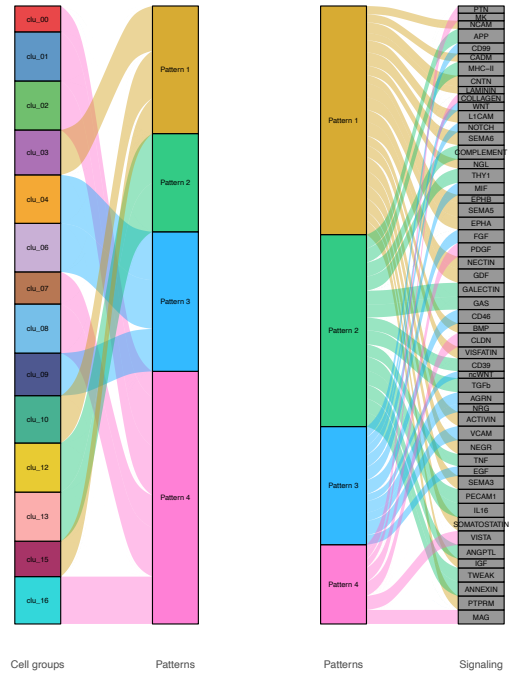
**C** Communication patterns

**Figure S4. Cell-to-cell communication in organoids. Related to Figure 3.**
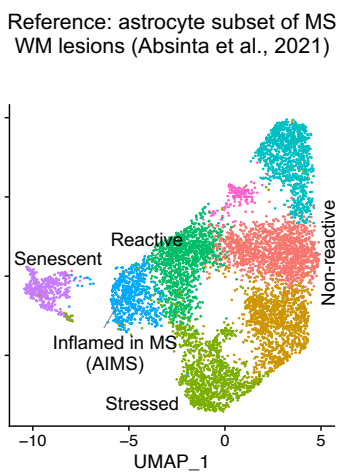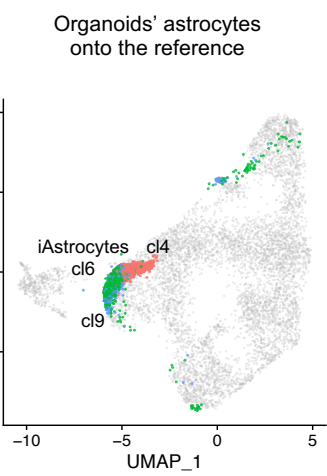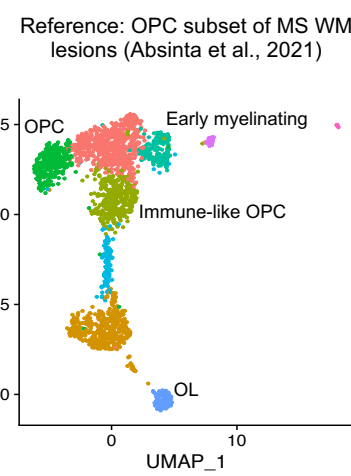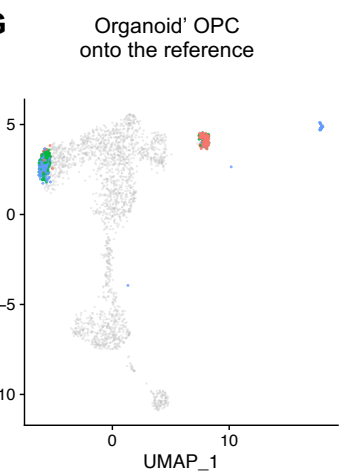(A) The inferred outgoing communication patterns of secreting cells, which shows the correspondence between the inferred latent patterns and cell groups, as well as signaling pathways. The thickness of the flow indicates the contribution of the cell group or signaling pathway to each latent pattern.
(B) The inferred incoming communication patterns of target cells that shows the correspondence between the inferred latent patterns and cell groups, as well as signaling pathways. The thickness of the flow indicates the contribution of the cell group or signaling pathway to each latent pattern.
(C) heatmap and dendrogram of the signaling pathways associated to the different cell patterns.

**A**

*NAMPT*
ANOVA p=0.03

*CXCL8*
ANOVA p=0.05

*AIF1*
ANOVA n.s.

*GFAP*
ANOVA n.s.

**B**

48 hour-Bulk Proteomics

*AIF1*
ANOVA n.s.

*GFAP*
ANOVA n.s.

**C**

GSEA enrichment score (hiMicroglia cl13 *vs* MIMS-iron)

Upregulated genes

Downregulated genes

**D**

Reference: astrocyte subset of MS WM lesions (Absinta et al., 2021)

**E**

Organoids' astrocytes onto the reference

**F**

Reference: OPC subset of MS WM lesions (Absinta et al., 2021)

**G**

Organoid' OPC onto the reference

**Figure S5. Transcriptomic and proteomic of MS-CSF inflamed organoids. Related to Figure 4.**

(A) Gene expression (normalized to *GAPDH* and untreated condition) of *NAMPT, CXCL8, AIF1,* and *GFAP* in 8-week-old organoids with hiMicroglia exposed to CSF from healthy subjects (*n*=3) and subjects with diagnosed MS (*n*=3; 2 primary progressive and 1 relapsing remitting), as determined by RT-qPCR (one-way ANOVA and multiple comparison) (*n*=4 RNA samples each consisting of ~200 organoids derived from 4 hiPSC lines).

(B) Heatmap and dendrogram relative to bulk proteomic analysis conducted on untreated (named "CTRL") vs 48h CSF-treated organoids (named "Treated").

(C) Gene set enrichment analysis (GSEA) performed in hiMicroglia (cluster 13) *vs* MIMS-iron for upregulated genes left) and downregulated (right) genes. The GSEA algorithm calculates an enrichment score reflecting the degree of overrepresentation at the top or bottom of the ranked list of the genes included in a gene set in a ranked list of all genes present in our scRNA-seq datasets. A positive enrichment score indicates gene set enrichment at the top of the ranked list; a negative enrichment score indicates gene set enrichment at the bottom of the ranked list.

(D) Reference atlas based on the re-analysis of astrocyte subclustering at the chronic active MS lesion in Absinta et al.[3].
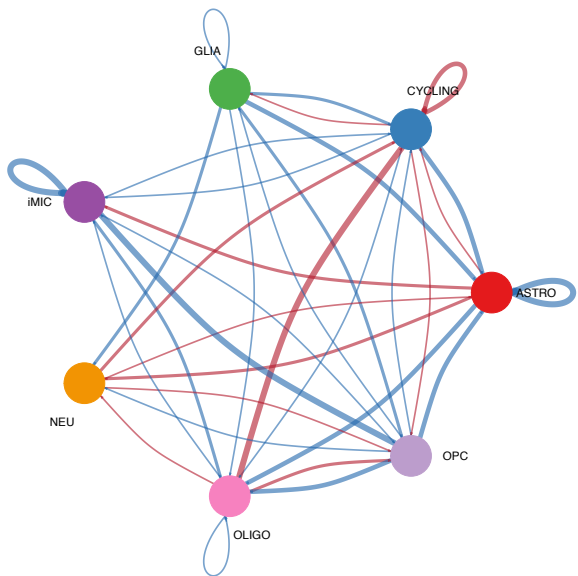
(E) Mapping of 3D organoid single cell data onto the MS astrocyte subset reference.

(F) Reference atlas was based on the re-analysis of Absinta et al.,[3] OPC subclustering at the chronic active MS lesion.
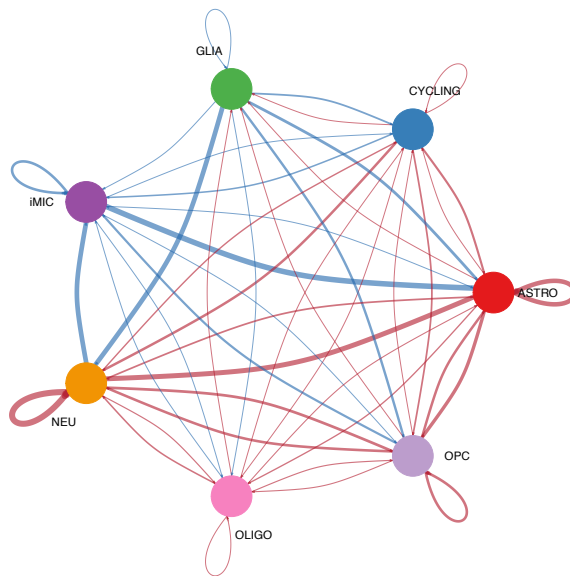
(G) Mapping of 3D organoids single cell data onto the MS OPC subset reference (F).

**A**

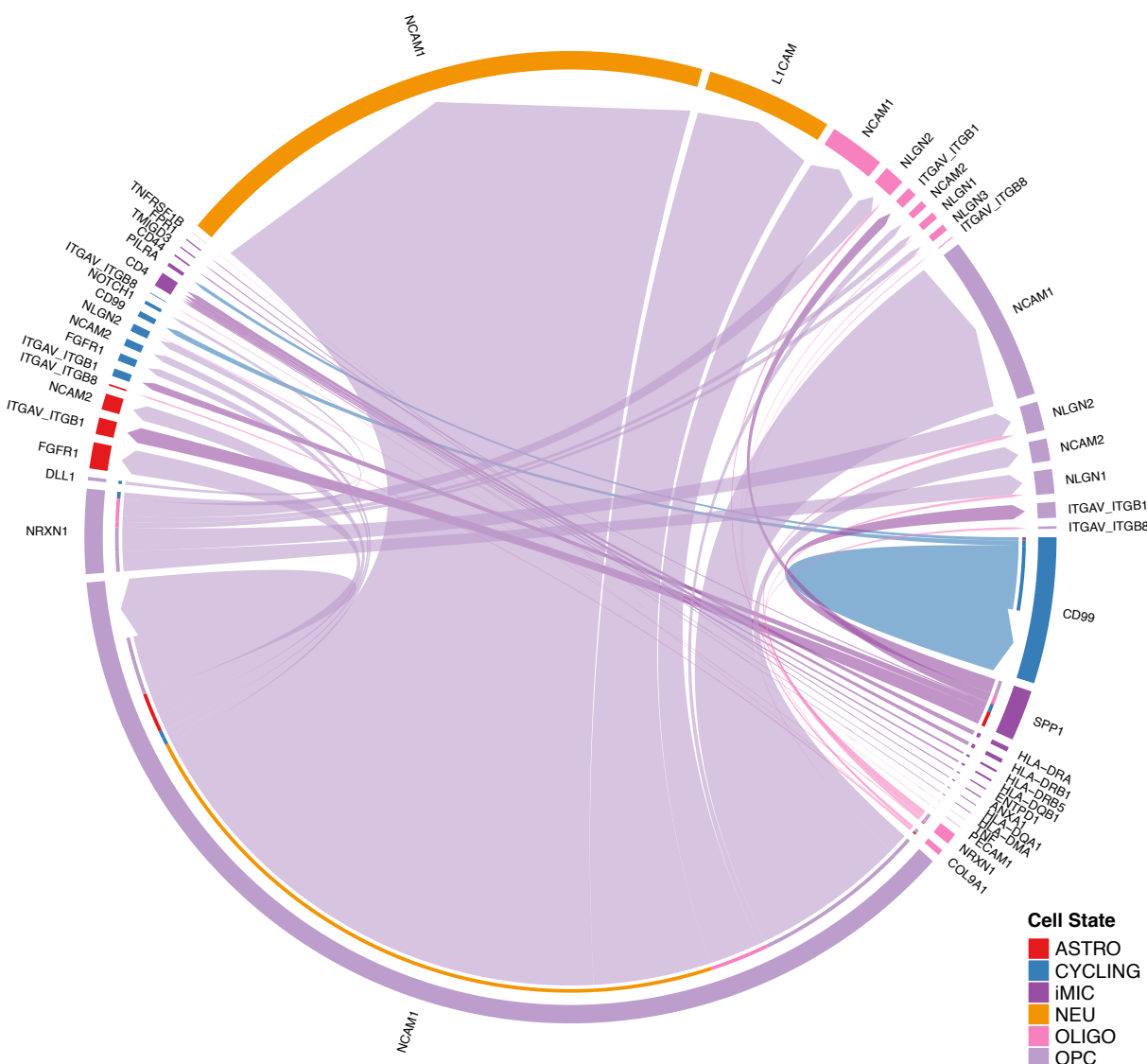CSF-treated vs untreated organoids
Differential number of interactions

CSF-treated vs untreated organoids
Differential interaction strength

**B**

Upregulated signaling in CSF-treated vs untreated organoids

**Cell State**
- ASTRO
- CYCLING
- iMIC
- NEU
- OLIGO
- OPC

**Figure S6. Cell-to-cell communication perturbation by MS-inflamed CSF. Related to Figure 4.**
(A) CellChat circle plots showing differential number of interactions and differential interaction strength in the crosstalk among cell populations of CSF-treated vs untreated organoids. Red lines indicate that the displayed communication is increased in CSF-treated organoids compared with untreated organoids, whereas blue lines indicate that the displayed communication is decreased in CSF-treated organoids. The line thickness is proportional to the number of interaction (circle plot on the left) or to the interaction strength (circle plot on the right).
(B) CellChat chord plot showing upregulated signaling in CSF-treated vs untreated organoids. The edge width is proportional to the indicated number of ligand-receptor pairs. Each cell population is color-coded.